Nanoscale Advances

ROYAL SOCIETY OF CHEMISTRY

PAPER

View Article Online
View Journal | View Issue

Cite this: *Nanoscale Adv.*, 2024, **6**, 1917

Controlling supramolecular copolymerization of alkynylplatinum(II) terpyridine complexes: from isodesmic to cooperative mechanisms†

Sehee Kim,‡ Minhye Kim,‡ Seojeong Woo, Juyeong Kim, Sung Ho Jung * and Jong Hwa Jung *

Recently, cooperative supramolecular polymerization has garnered considerable attention due to its significant potential for enabling controlled chain-growth polymerization, which offers a route to achieving a well-defined degree of polymerization and low polydispersity. In this study, we synthesized two distinct alkynylplatinum(II) complexes, one bearing a saturated long alkyl chain (**Pt-Sat-C18**) and another containing a diacetylene moiety within a long alkyl chain (**Pt-DA-C25**). Spectroscopic analyses revealed that **Pt-Sat-C18** undergoes supramolecular polymerization *via* an isodesmic pathway, while **Pt-DA-C25** assembles cooperatively. Intriguingly, the mechanism of supramolecular copolymerization could be tuned by varying the composition ratios: transitioning from an isodesmic to a cooperative pathway was achieved by increasing the proportion of **Pt-DA-C25**. Moreover, UV irradiation prompted a shift from an isodesmic to a cooperative assembly mechanism. Morphologically, self-assembled **Pt-Sat-C18** resulted in left-handed fibrillar structures, whereas **Pt-DA-C25** led to left-handed tubular assemblies. Supramolecular co-assembly further revealed helical ribbon or tubular structures. Photoluminescent properties were also observed, with emission spectra centered at approximately 650 nm, attributed to the formation of excimer species facilitated by strong Pt···Pt interactions. To elucidate the mechanisms underlying these supramolecular polymerizations, temperature-dependent UV-visible spectroscopy was conducted during the cooling/heating processes, and thermodynamic parameters for both isodesmic and cooperative pathways were quantitatively assessed through curve fitting.

Received 22nd December 2023
Accepted 28th February 2024

DOI: 10.1039/d3na01140b

rsc.li/nanoscale-advances

Introduction

The rational design of monomers capable of self-assembling into dynamically well-ordered structures is critical for the deployment of self-assembled materials across various applications.[1–16] Achieving this goal necessitates the precise control of molecular interactions like solvophobic effects, π–π stacking, and intermolecular hydrogen bonding in the realm of supramolecular polymerization. For supramolecular polymers, even minor alterations in molecular structure can result in significant, often unpredictable, changes in the structural and dynamic behavior of aggregates.[17–25] Consequently, the rational design of supramolecular polymers remains a formidable challenge, underscoring the need for an in-depth understanding of the intermolecular interactions that drive self-assembly.

In the formation of supramolecular polymers from small molecular building blocks, two primary growth mechanisms are observed: the so-called isodesmic[26–28] and cooperative[29–39] pathways. In the isodesmic mechanism, the aggregation behavior generally follows a step-growth mechanism, displaying high polydispersity and a degree of polymerization contingent upon a single binding constant.[40,41] No distinct transition point neither a critical concentration nor a critical temperature, resulting in an approximate transition from a monomeric to a polymeric state. On the other hand, the cooperative mechanism involves a two-step process governed by two distinct binding constants: nucleation (K_n) and elongation (K_e).[42,43] This mechanism is characterized by a lower degree of polydispersity and exhibits a sharp transition point from nucleation to elongation regime, observable at a critical concentration or temperature, unlike the isodesmic mechanism.

Recently, cooperative supramolecular polymerization has garnered significant attention due to its potential for controlled chain growth, leading to high degrees of polymerization, low dispersity, and controllable morphologies. Consequently, the design of the building blocks emerges as a pivotal factor for realizing desired supramolecular polymers with potential

Department of Chemistry, Research Institute of Natural Sciences, Gyeongsang National University, Jinju 52828, Korea. E-mail: shjung@gnu.ac.kr; Jonghwa@gnu.ac.kr

† Electronic supplementary information (ESI) available. See DOI: https://doi.org/10.1039/d3na01140b

‡ These authors contributed equally.

applications in material science and supramolecular chemistry.[44–55]

Platinum(II) complexes with tridentate π-acceptor ligands are recognized for their outstanding spectroscopic properties and a strong propensity to form supramolecular architectures through Pt⋯Pt and π–π interactions, both in solid and solution states, due to their square-planar configuration.[56–73] This has led to significant interest in supramolecular structures based on Pt(II) complexes, driven by their inherently fascinating physical properties and the diverse morphologies of self-assembled structures. For instance, V. W. W. Yam and coworkers reported various morphologies of supramolecular aggregates derived from mono- and binuclear platinum(II) complexes, including helical fibers, tubular, and ribbon formations, alongside their spectroscopic characteristics.[74,75] They further elucidated the formation mechanisms of these supramolecular structures of platinum(II) complex through alterations in solvent composition. The supramolecular assembly in aqueous solutions follows an isodesmic model, whereas in acetone and H_2O (7 : 1 v/v), it adopts a cooperative growth strategy, characterized by nucleation and elongation mechanisms.[76] Furthermore, exploring Pt(II) complex systems that transition from isodesmic to cooperative supramolecular copolymerization remains a significant challenge. In this work, we report the mechanisms underlying supramolecular copolymerization based on **Pt-Sat-C18** and **Pt-DA-C25** at varying composition ratios. The copolymerization mechanism was regulated *via* UV-irradiation, resulting in pronounced morphological changes influenced by composition ratios. Thermodynamic studies further corroborated the self-assembly mechanisms of both isodesmic and cooperative supramolecular copolymers. Pt(II) complex-based supramolecular polymers can diverse applicative potential spanning molecular recognition, pH sensing and biomolecular labeling, due to special photophysical characteristics.[63]

Results and discussion

Preparation of ligands

As shown in Scheme S1,† chiral terpyridine ligands, **Pt-Sat-C18** and **Pt-DA-C25** (Fig. 1), were synthesized *via* distinct multi-step routes. The synthesis commenced with the preparation of chiral precursor **2**, containing an *S*-alanine moiety, according to a previously reported procedure.[77,78] Compound **3** was subsequently synthesized through the reaction of precursor **2** with decanedioyl dichloride and triethylamine in dichloromethane (DCM). The subsequent stage involved the formation of platinum(II) complex **4**, achieved by reacting compound **3** with dichloro(1,5-cyclooctadiene)platinum(II) in a water–methanol mixture. The target ligand **Pt-Sat-C18** was then obtained by reacting complex **4** with phenylacetylene that featured a saturated long alkyl chain, employing DCM as the solvent. In a parallel synthesis, **Pt-DA-C25** was synthesized employing a methodology analogous to that used for **Pt-Sat-C18**, with the key distinction being the utilization of a diacetylene moiety in the long alkyl chain. Comprehensive characterization of all synthesized products was conducted using nuclear magnetic resonance (NMR) spectroscopy, infrared (IR) spectroscopy, and electrospray ionization mass spectrometry (ESI-MS).

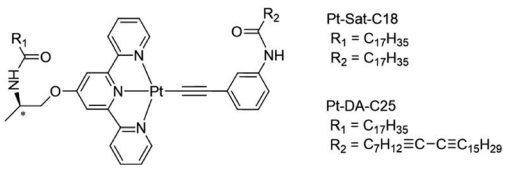

Fig. 1 Chemical structures of building blocks used in this works.

Spectroscopic studies of supramolecular polymer

To explore the formation of supramolecular polymers in mixed solvents of dimethyl sulfoxide (DMSO) and H_2O, UV-vis spectral changes of **Pt-Sat-C18** and **Pt-DA-C25** ligands were measured in varying DMSO/H_2O ratios. Optimal conditions for supramolecular polymerization were identified as a 5 : 1 (v/v) mixture of DMSO and H_2O. As depicted in Fig. 2A, both **Pt-Sat-C18** and **Pt-DA-C25** displayed nearly identical absorption spectra, characterized by intense high-energy absorption bands in the 250–320 nm region. These bands are attributed to intraligand [π → π*] transitions within the terpyridine units. Additionally, absorption bands appearing between 450–490 nm were identified, indicative of a metal-to-ligand charge transfer (MLCT) [dπ(Pt) → π*(terpyridine)] transition, compounded with a ligand-to-ligand charge transfer (LLCT) [π(terpyridine) → π*(terpyridine)] character. Notably, in the mixed DMSO and H_2O (5 : 1 v/v), a distinct absorption feature was observed in the 520–560 nm range. This phenomenon is ascribed to a metal–metal-to-ligand charge transfer (MMLCT) transition, implicating Pt⋯Pt interactions during the course of supramolecular polymerization. In stark contrast, this MMLCT-associated absorption band was conspicuously absent when the ligands were dissolved in pure DMSO (Fig. S1A†), signifying the absence of Pt⋯Pt interactions under these solvent conditions.

To further substantiate the role of metal–metal-to-ligand charge transfer (MMLCT) in supramolecular polymerization, photoluminescence spectra of **Pt-Sat-C18** and **Pt-DA-C25** were acquired in both a mixed DMSO/H_2O solvent system (5 : 1, v/v) and in pure DMSO (Fig. 2B and S1B†). Notably, both **Pt-Sat-C18** and **Pt-DA-C25** manifested intense emission bands at approximately 650 nm (Fig. 2B). These bands are consistent with the formation of excimer species during supramolecular polymerization.[79] A characteristic emission band associated with MMLCT was identified at approximately 610 nm in the context of supramolecular polymerization.[69] Emission bands at longer wavelengths were ascribed to robust Pt⋯Pt interactions, as compared to those in previously reported compounds.[69,70] Contrastingly, in pure DMSO, emission bands were observed at approximately 560 nm (Fig. S1B†), attributable to metal-to-ligand charge transfer (MLCT). These findings corroborate the monomeric nature of **Pt-Sat-C18** and **Pt-DA-C25** in a DMSO-only environment. Further credence to this supramolecular polymerization mechanism was lent by circular dichroism (CD) spectroscopy. Pronounced negative CD bands were detected in

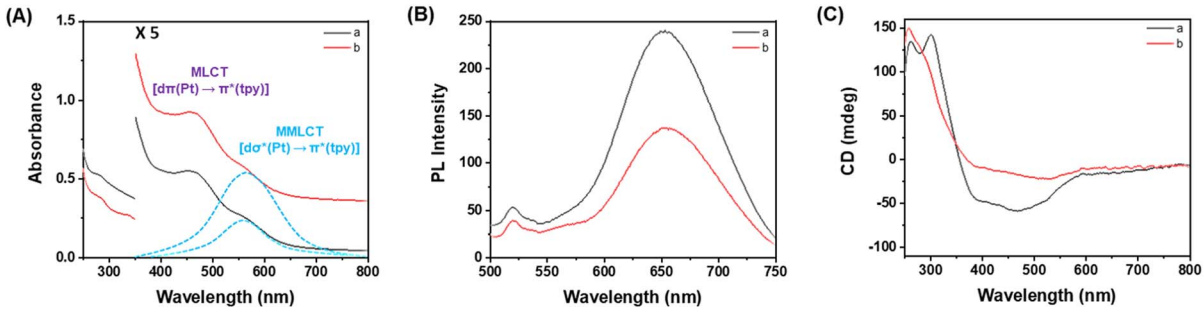

Fig. 2 (A) UV-vis, (B) PL and (C) CD spectra of (a) **Pt-Sat-C18** (300 μM) and (b) **Pt-DA-C25** (300 μM) in a mixed DMSO and H_2O (5 : 1 v/v): the spectra with dot lines in (A) were obtained by curve fitting.

the 350–600 nm range (Fig. 2C), arising from MLCT and metal–metal charge transfer (MMCT) processes during supramolecular polymerization. The negative CD signals indicative that **Pt-Sat-C18** and **Pt-DA-C25** form supramolecular polymers with left-handed screw shape. In addition, the strong positive CD band showed at around 300 nm, corresponding to π → π* transitions within the terpyridine unit. These observations imply the formation of helical structures in the supramolecular polymers of **Pt-Sat-C18** and **Pt-DA-C25**. These CD signals also originate from helical supramolecular polymers induced by the *S*-enantiomeric moiety of building blocks. Notably, no CD signals were observed in pure DMSO (Fig. S1C†), corroborating the absence of supramolecular polymerization and reinforcing the monomeric existence of these Pt(II) complexes. Hence, our results confirm that **Pt-Sat-C18** and **Pt-DA-C25** engage in supramolecular polymerization when dissolved in a mixture of DMSO/H_2O (5 : 1, v/v).

To elucidate the role of intermolecular hydrogen bonding in the assembly of supramolecular nanostructures, Fourier transform infrared (FT-IR) spectroscopy was employed. When compared to the spectra of monomeric **Pt-Sat-C18** and **Pt-DA-C25** dissolved in pure DMSO, the FT-IR spectra of the aggregates in a DMSO/H_2O mixture (5 : 1, v/v, 1 mM) exhibited a discernible shift in the –NH stretching bands toward lower wavenumbers (Fig. S2†). This shift serves as a clear indicator of the formation of intermolecular hydrogen bonds involving the amide functional groups. Supplementing these observations, ^{1}H NMR studies performed in DMSO-d_6 and D_2O (5 : 1, v/v) at 298 K showed broadening of the aromatic proton peaks for both **Pt-Sat-C18** and **Pt-DA-C25** (Fig. S3†), a feature ascribed to the assembly of these molecules into supramolecular polymers. Conversely, at elevated temperature (363 K), these aromatic proton peaks displayed more pronounced low-field shifts and improved resolution, signifying the disassembly into monomeric species. Taken together, these FT-IR and ^{1}H NMR spectral data strongly support the notion that intermolecular hydrogen bonding, along with π–π stacking interactions, serve as the principal driving forces underlying the formation of these supramolecular polymers.

Supramolecular polymerization

To gain a nuanced understanding of self-assembly behavior, we conducted temperature-dependent UV-vis spectroscopic measurements on **Pt-Sat-C18** and **Pt-DA-C25**. These measurements were performed under a controlled temperature change of 1 K min^{-1} in a DMSO/H_2O mixture (5 : 1, v/v). For **Pt-Sat-C18**, a sigmoidal curve was observed when monitoring absorption intensities at 270 and 550 nm (Fig. 3 and S4†). During the cooling process, the absorption intensity at 550 nm, attributable to metal–metal-to-ligand charge transfer (MMLCT), displayed an increase below 350 K. This observation implies the activation of MMLCT interactions during supramolecular polymerization at below 350 K temperature. Intriguingly, both heating and cooling curves manifested a well-defined sigmoidal shape, with no hysteresis observed (Fig. 3C). These features suggest that **Pt-Sat-C18** undergoes supramolecular polymerization *via* an isodesmic model. In contrast, the cooling curve for **Pt-DA-C25** demonstrated a distinctly non-sigmoidal profile (Fig. 3B, D and S5†), indicative of a cooperative self-assembly mechanism featuring successive nucleation and elongation stages. These results indicate that the supramolecular polymers based on **Pt-Sat-C18** follow a distinct pathway compared to their **Pt-DA-C25** counterpart, likely due to the greater hydrophobicity

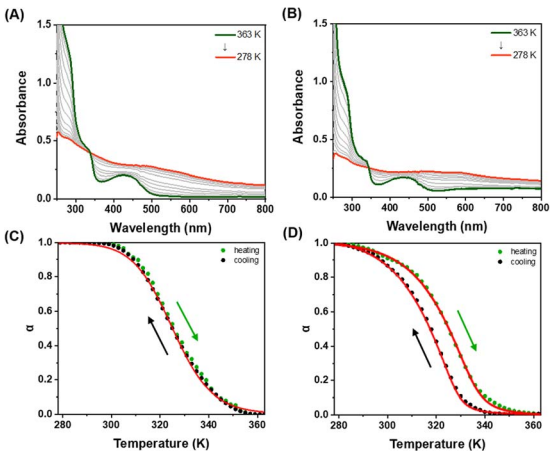

Fig. 3 Temperature-dependent UV-vis spectral changes of (A) **Pt-Sat-C18** (300 μM) and (B) **Pt-DA-C25** (300 μM) in DMSO and H_2O (5 : 1 v/v). Plots for α_{agg} *vs.* temperatures of (C) **Pt-Sat-C18** and (D) **Pt-DA-C25** upon heating and cooling at a rate of 1 K min^{-1} in DMSO and H_2O (5 : 1 v/v) at 270 nm. The cooperativity parameter σ, representing the ratio of K_n/K_e, was approximately 1 for the self-assembled **Pt-Sat-C18** and 4.5 × 10^{-3} (during cooling) and 1.3 × 10^{-2} (during heating) for the self-assembled **Pt-DA-C25**, respectively. These values were obtained through curve fitting with Matlab.

of the latter and differences in molecular arrangement during supramolecular polymerization. Additionally, we calculated the number-averaged degree of polymerization,[41] DP_N, for **Pt-Sat-C18** and **Pt-DA-C15** (Fig. S6†). As shown in Fig. S6,† the number-averaged degree of polymerization for **Pt-DA-C25** is higher than that of **Pt-Sat-C18** at temperatures below 290 K, indicating that the formation mechanism of **Pt-DA-C25** differs from that of **Pt-Sat-C18**. Corroborating these observations, temperature-dependent circular dichroism (CD) spectral changes were consistent with the UV-vis data (Fig. S7 and S8†). Further supporting these findings, photoluminescence (PL) intensity at 650 nm diminished progressively, while the PL band at 560 nm increased (Fig. S9 and S10†). This behavior is consistent with the dissociation of the MMLCT-driven supramolecular polymers into monomeric species.

Supramolecular copolymerization by different composition ratios

To explore the intricacies of supramolecular copolymerization, we examined various composition ratios of **Pt-Sat-C18** to **Pt-DA-C25** in a DMSO/H_2O mixture (5 : 1, v/v) (Fig. S13–S18†). Upon cooling, the absorbance changes for supramolecular copolymers formed at 9 : 1 and 8 : 2 ratios of **Pt-Sat-C18** to **Pt-DA-C25** displayed sigmoidal curves similar to those observed for **Pt-Sat-C18** alone (Fig. 4). This evidence points toward the dominance of an isodesmic mechanism for copolymers wherein **Pt-Sat-C18** constitutes the major component. Conversely, copolymers formulated at 4 : 6, 6 : 4, and 2 : 8 ratios (**Pt-Sat-C18** to **Pt-DA-C25**) manifested non-sigmoidal cooling curves (Fig. 4). Further quantitative analysis yielded cooperativity parameter σ as the ratio of K_n/K_e ranging from 1.7×10^{-2} to 2.1×10^{-2},[26] obtained *via* curve fitting with Matlab. These observations suggest a transition toward a cooperative assembly mechanism in these copolymer systems. In a mixture of **Pt-Sat-C18 : Pt-DA-C25**, the nucleation of **Pt-DA-C25** proceeds rapidly compared to the supramolecular polymerization of **Pt-Sat-C18**. The nucleation of **Pt-DA-C25** would act as a seed for the elongation of **Pt-Sat-C18** and **Pt-DA-C25**, leading to a cooperative pathway. In the co-assembly process, both **Pt-Sat-C18** and **Pt-DA-C25** undergo co-assembled nucleation under competitive pathways, leading to a cooperative mechanism. Consequently, as a result of this nucleation formation process, the isodesmic mechanism is transformed into a cooperative mechanism to form a supramolecular copolymer. Notably, the mechanism underlying copolymer formation appears to be readily tunable by adjusting the compositional ratios of the constituent building blocks. Such control is imperative for generating supramolecular copolymers *via* a cooperative mechanism, which is particularly relevant for the kinetic stabilization of metastable states in the synthesis of multi-block supramolecular copolymers.

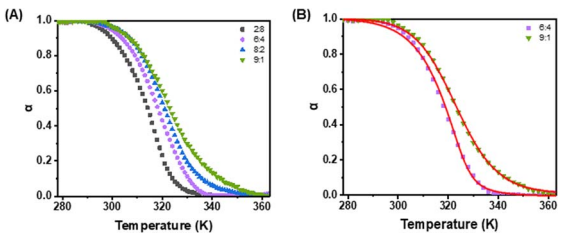

Fig. 4 (A) Plots of α_{agg} against temperature for supramolecular copolymers (300 μM) at different composition ratios of Pt-Sat-C18 and Pt-DA-C25 (2 : 8, 6 : 4, 8 : 2 and 9 : 1) at 270 nm. (B) Fitting curve of self-coassembled polymers at different composition ratios (6 : 4 and 9 : 1) of Pt-Sat-C18 and Pt-DA-C25; the composition ratio of 6 : 4 suggests a cooperative pathway, while the composition ratio of 9 : 1 indicates an isodesmic pathway.

Subsequently, we probed the role of UV-irradiation in governing the mechanism of supramolecular polymerization. When the supramolecular polymer based on **Pt-DA-C25** was cooled in a DMSO and H_2O mixture (5 : 1 v/v), a non-sigmoidal cooling curve was observed irrespective of UV-irradiation duration (Fig. S11†). Remarkably, a transition in absorbance behavior was witnessed for co-assembled polymers formed at a 9 : 1 ratio of **Pt-Sat-C18** to **Pt-DA-C25** upon UV-irradiation for 30 min during the cooling process (Fig. S12 and S13†). These data suggest that UV-irradiation shifts the co-assembled polymer system toward a cooperative assembly pathway, characterized by nucleation–elongation mechanics. We also examined the FT-Raman spectral changes in both the self-assembled pure **Pt-DA-C25** and the coassembly of **Pt-Sat-C18** and **Pt-DA-C25** (at a 9 : 1 ratio) to verify the occurrence of 1,4-addition polymerization of the diacetylene moiety under UV irradiation (Fig. S19†). Prior to irradiation, the self-assembled pure **Pt-DA-C25** exhibited vibrational bands at 2083 cm^{-1} and 1458 cm^{-1} ($\nu_{C\equiv C}$). After 30 minutes of irradiation with Hg lamp (Fig. S17A†), the vibrational band at 1458 cm^{-1} for the diacetylene group shifted to a higher wavenumber, corresponding to the –C=C– stretching vibrational region.[80] Additionally, the peak at 2083 cm^{-1} shifted to a shorter wavenumber, indicating increased conjugation (Fig. S20†). These results confirm the effective polymerization of the self-assembled pure **Pt-DA-C25** under UV irradiation.

In contrast, following UV irradiation of the coassembly formed at a 9 : 1 ratio of **Pt-Sat-C18** to **Pt-DA-C25**, the vibrational band at 1458 cm^{-1} exhibited a weak shift compared to the self-assembled pure **Pt-DA-C25** (Fig. S19B†). This observation suggests that the 1,4-addition reaction of diacetylene moieties in the coassembly does not occur as effectively as in the self-assembled pure **Pt-DA-C25**. Notably, these findings unveil the capacity to modulate the assembly mechanism of supramolecular polymers featuring UV-responsive functional groups. Therefore, UV-irradiation emerges as a powerful tool for dictating the structural attributes of complex supramolecular architectures.

Morphology observation of supramolecular polymers

Morphological characterization of the self-assembled polymers of **Pt-Sat-C18** and **Pt-DA-C25** in a mixed solvent of DMSO and H_2O (5 : 1 v/v) was conducted *via* scanning electron microscopy (SEM) and transmission electron microscopy (TEM) (Fig. 5). For **Pt-Sat-C18**, SEM images revealed a well-defined left-handed helical fiber architecture with an approximate diameter of 75 nm (Fig. 5A). Conversely, **Pt-DA-C25** exhibited a tubular

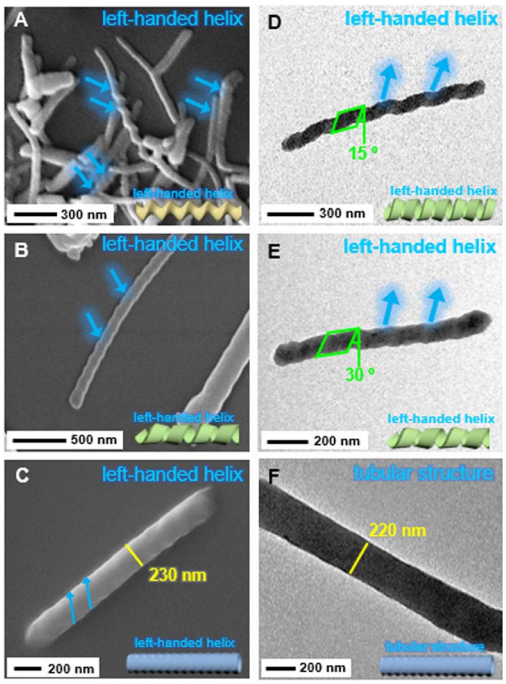

Fig. 5 SEM and TEM images of the self-assembled polymers obtained by (A) pure **Pt-Sat-C18**, (B and E) 8 : 2 and (D) 4 : 6 ratios of **Pt-Sat-C18** and **Pt-DA-C25** and pure (C and F) **Pt-DA-C25** in DMSO and H_2O (5 : 1 v/v).

morphology, which was additionally confirmed to feature a left-handed helical twist by SEM and TEM images (Fig. 5C and F). Intriguingly, supramolecular copolymers comprising different ratios of **Pt-Sat-C18** and **Pt-DA-C25** (8 : 2 and 4 : 6) manifested left-handed helical tubular or ribbon-like morphologies with diameters around 110–120 nm. Notably, a 4 : 6 ratio coassembly of **Pt-Sat-C18** and **Pt-DA-C25** yielded a left-handed helical ribbon structure (Fig. 5D), suggesting a morphological transition from a left-handed tubular arrangement. These findings underscore the critical role of the **Pt-DA-C25** composition ratio in modulating the resulting morphologies. Additionally, the TEM image in Fig. 5F revealed a clear inner hollow cavity a diameter of approximately 220 nm. In general, the tubular structure in the self-assembling process begins with small vesicular structures.[81] Vesicles then grow into ribbon structures. Subsequently, the ribbon structure transforms into a helical tubular structure.[81] In this study, the vesicular structure was not observed, which may be due to the rapid morphological transformation in supramolecular polymerization. The tubular structures in Fig. 5 could also originate from small vesicles. Therefore, we conclude that the structural attributes of coassembled polymers can be strategically tuned *via* altering the composition ratios of **Pt-Sat-C18** and **Pt-DA-C25**.

Thermodynamic study of supramolecular polymers

The temperature-dependent UV-vis spectral changes of **Pt-Sat-C18** and **Pt-DA-C25** (200–600 μM) at ranges of various concentrations were observed by cooling process at a rate of 1 K min^{-1} in DMSO and H_2O (5 : 1 v/v) (Fig. 6 and S21–S28†). As mentioned early, since the plots of the fraction of aggregated **Pt-Sat-C18** molecules (α_{agg}) against temperature for supramolecular polymers based on **Pt-Sat-C18** showed sigmodal shapes, the thermodynamic parameters (ΔG, ΔH and ΔS) were calculated by applying isodesmic model (Fig. 6A and B). The binding constant (K_I) and Gibbs free energy (ΔG) were calculated to be in the range of 2.6×10^4 to 1.3×10^3 mol^{-1} and −29.3 kJ mol^{-1} at 298 K (Tables S1 and S2†), respectively. On the other hand, the plots of α_{agg} against temperature for supramolecular polymer based **Pt-DA-C25** showed non-sigmodal curves (Fig. 6C). Through curve fitting by Matlab using basis on cooperative model with a nucleation and elongation mechanism (Fig. 6C and D), the ΔG_e, ΔH_e and the elongation binding constant (K_e) afforded −24.3 kJ mol^{-1} at 298 K, −43.0 kJ mol^{-1} and 1.8×10^4 mol^{-1} (Table S3†), respectively.

The thermodynamic parameters of co-assembled polymers formed at different composition ratios of **Pt-Sat-C18** and **Pt-DA-C25** (9 : 1 to 2 : 8) were also calculated by curve fitting obtained in the cooling process at a rate of 1 K min^{-1} in DMSO and H_2O (5 : 1 v/v). The ΔG_e of co-assembled polymers formed at different composition ratios was −16.8 to −19.7 kJ mol^{-1} at 298 K (Table S4†), which was smaller than those obtained by **Pt-Sat-C18** and **Pt-DA-C25**. In addition, the ΔG_e decreased by increase of concentration of **Pt-Sat-C18**. This decrease of ΔG_e would due to mismatching between two building blocks in formation of supramolecular copolymers. Furthermore, the ΔG_e of the self-assembled **Pt-DA-C25** (−18.8 kJ mol^{-1} at 298 K) and co-assembly formed at 9 : 1 ratio (−17.1 kJ mol^{-1} at 298 K) after UV-irradiation for 30 min were smaller than that the self-assembly before UV-irradiation (Tables S5 and S6†), indicating leading disordering of supramolecular structure in 1,4-addition polymerization process of diacetylene moieties (Fig. S20†). Although UV irradiation did not influence the formation mechanism in the self-assembled **Pt-DA-C25** process, the ΔG_e of

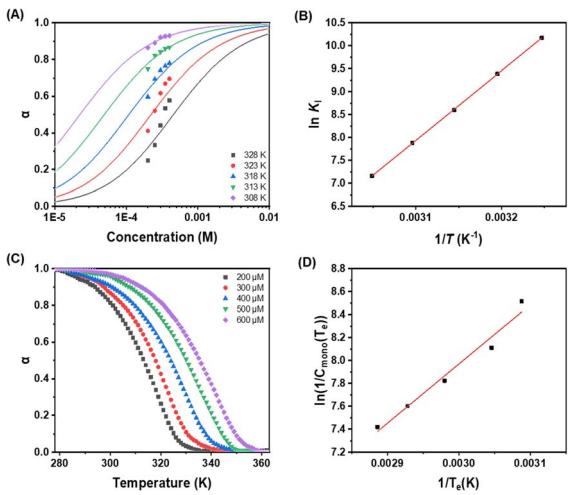

Fig. 6 (A) Plots of α_{agg} *vs.* concentration of **Pt-Sat-C18** in DMSO and H_2O (5 : 1 v/v) at different temperatures and corresponding isodesmic fit. (B) Van't Hoff plot for **Pt-Sat-C18** in DMSO and H_2O (5 : 1 v/v). (C) Plots of **Pt-DA-C25** for α_{agg} *vs.* temperature in DMSO and H_2O (5 : 1 v/v) at different concentrations. (D) Van't Hoff plot for **Pt-DA-C25** in DMSO and H_2O (5 : 1 v/v).

self-assembled **Pt-DA-C25** after UV irradiation (ΔG_e = −18.8 kJ mol^{-1}) significantly reduced compared to before UV irradiation (ΔG_e = −24.3 kJ mol^{-1}). This reduction was attributed to the disordering of the self-assembly. In contrast, the ΔG_e of the co-assembly of **Pt-Sat-C18** and **Pt-DA-C25** (9 : 1) was not influenced by UV irradiation (Tables S4 and S6†). However, the assembly mechanism shifted from isodesmic to cooperative. This change is attributed to a small amount of **Pt-DA-C25** undergoing a 1,4-addition reaction upon UV irradiation, leading to co-assembled nucleation through competitive pathways. In particular, exposure to UV irradiation caused a transition from an isodesmic to a cooperative assembly mechanism. This finding implies that UV irradiation offers a novel approach to controlling the self-assembly process.

Conclusions

We have precisely modulated the formation mechanisms of supramolecular polymers derived from alkyne platinum(II) complexes, each with either a saturated or unsaturated alkyl chain. Photoluminescence spectra of these chiral supramolecular polymers and copolymers prominently feature peaks around 650 nm, attributable to the generation of excimer species facilitated by robust Pt···Pt interactions. Notably, **Pt-Sat-C18** undergoes polymerization *via* an isodesmic pathway, whereas **Pt-DA-C25** favors a cooperative mechanism incorporating nucleation and elongation stages. Intriguingly, the innate isodesmic polymerization pathway of **Pt-Sat-C18** transitions to a cooperative mechanism in the presence of **Pt-DA-C25**, underscoring the capacity for dynamic control over supramolecular polymerization mechanisms. Morphological studies further support these mechanistic insights. Supramolecular polymers based on **Pt-Sat-C18** manifest as helical fibers, whereas copolymers derived from varying composition ratios of **Pt-Sat-C18** and **Pt-DA-C25** adopt either left-handed ribbon or tubular—morphologies reminiscent of the supramolecular polymers based on **Pt-DA-C25** alone. Furthermore, UV irradiation prompted a shift from an isodesmic to a cooperative assembly mechanism. These findings not only demonstrate the feasibility of controlling the self-assembly mechanisms of supramolecular polymers but also offer an innovative strategy for dictating morphology in supramolecular copolymerization processes.

Conflicts of interest

There are no conflicts to declare.

Acknowledgements

This research was supported by a National Foundation of Korea (NRF) grant funded by the Korean Government (MSIT) (2021R1A2C2007664 and 2022R1A4A1022252).

Notes and references

1 E. Krieg and B. Rybtchinski, Noncovalent water-based materials: robust yet adaptive, *Chem.–Eur. J.*, 2011, **17**, 9016–9026.
2 S. I. Stupp, Self-assembly and biomaterials, *Nano Lett.*, 2010, **10**, 4783–4786.
3 Y. Wang, T. Hasegawa, H. Matsumoto, T. Mori and T. Michinobu, Rational design of high-mobility semicrystalline conjugated polymers with tunable charge polarity: beyond benzobisthiadiazole-based polymers, *Adv. Mater.*, 2017, **27**, 1604608.
4 P. Liebing, L. Wang, J. W. Gilje, L. Hilfert and F. T. Edelmann, Supramolecular first-row transition metal complexes of 3-(3,5dimethylpyrazol-1-yl)propanamide: three different coordination modes, *Polyhedron*, 2019, **164**, 228–235.
5 M. J. Webber, E. A. Appel, E. W. Meijer and R. Langer, Supramolecular biomaterials, *Nat. Mater.*, 2016, **15**, 13–26.
6 M. Gao, D. Kwaria, Y. Norikane and Y. Yue, Visible-light-switchable azobenzenes: molecular design, supramolecular systems, and applications, *Nat. Sci.*, 2022, **3**, e220020.
7 H. Han, D. Zhang, Z. Zhu, R. Wei, X. Xiao, X. Wang, Y. Liu, Y. Ma and D. Zhao, Aromatic stacking mediated spin-spin coupling in cyclophane-assembled diradicals, *J. Am. Chem. Soc.*, 2021, **143**, 17690–17700.
8 J. Tong, L. M. Jia, P. Shang and S. Y. Yu, Controlled synthesis of supramolecular architectures of homo- and heterometallic complexes by programmable self-assembly, *Cryst. Growth Des.*, 2019, **19**, 30–39.
9 K. K. Kartha, N. K. Allampally, S. Yagai, R. Q. Albuquerque and G. Fernandez, Mechanistic insights into the self-assembly of an acid-sensitive photoresponsive supramolecular polymer, *Chem.–Eur. J.*, 2019, **25**, 9230–9236.
10 R. W. Saalfrank, H. Maid and A. Scheurer, Supramolecular coordination chemistry: the synergistic effect of serendipity and rational design, *Angew. Chem., Int. Ed.*, 2008, **47**, 8794–8824.
11 L. Zhou, L. Xu, X. Song, S. M. Kang, N. Liu and Z. Q. Wu, Nickel(II)-catalyzed living polymerization of diazoacetates toward polycarbene homopolymer and polythiophene-block-polycarbene copolymers, *Nat. Commun.*, 2022, **13**, 811.
12 M. H. Chan and V. W. Yam, Toward the design and construction of supramolecular functional molecular materials based on metal-metal interactions, *J. Am. Chem. Soc.*, 2022, **144**, 22805–22825.
13 N. Baumer, J. Matern and G. Fernandez, Recent progress and future challenges in the supramolecular polymerization of metal-containing monomers, *Chem. Sci.*, 2021, **12**, 12248–12265.
14 L. Xu, C. Wang, Y. X. Li, X. H. Xu, L. Zhou, N. Liu and Z. Q. Wu, Crystallization-driven asymmetric helical assembly of conjugated block copolymers and the aggregation induced white-light emission and circularly polarized luminescence, *Angew. Chem., Int. Ed.*, 2020, **59**, 16675–16682.
15 C. Wang, L. Xu, L. Zhou, N. Liu and Z. Q. Wu, Asymmetric living supramolecular polymerization: precise fabrication of one-handed helical supramolecular polymers, *Angew. Chem., Int. Ed.*, 2022, **61**, e202207028.
16 N. Liu, R. T. Gao and Z. Q. Wu, Helix-induced asymmetric self-assembly of pi-conjugated block copolymers: from

controlled syntheses to distinct properties, *Acc. Chem. Res.*, 2023, **56**, 2954–2967.
17 F. Wang, R. Liao and F. Wang, Pathway control of pi-conjugated supramolecular polymers by incorporating donor-acceptor functionality, *Angew. Chem., Int. Ed.*, 2023, **62**, e202305827.
18 S. A. Lim, S. H. Jung and J. H. Jung, Kinetically controlled chiral metal-coordinated supramolecular polymerization accompanying helical inversion or morphological transformation, *Bull. Korean Chem. Soc.*, 2023, **44**, 322–331.
19 D. Bochicchio, M. Salvalaglio and G. M. Pavan, Into the dynamics of a supramolecular polymer at submolecular resolution, *Nat. Commun.*, 2017, **8**, 147.
20 M. B. Baker, L. Albertazzi, I. K. Voets, C. M. Leenders, A. R. Palmans, G. M. Pavan and E. W. Meijer, Consequences of chirality on the dynamics of a water-soluble supramolecular polymer, *Nat. Commun.*, 2015, **6**, 6234.
21 S. Yadav, A. K. Sharma and P. Kumar, Nanoscale self-assembly for therapeutic delivery, *Front. Bioeng. Biotechnol.*, 2020, **8**, 127.
22 X. Zhu, Y. Jiang, D. Yang, L. Zhang, Y. Li and M. Liu, Homochiral nanotubes from heterochiral lipid mixtures: a shorter alkyl chain dominated chiral self-assembly, *Chem. Sci.*, 2019, **10**, 3873–3880.
23 Y. Imai and J. Yuasa, Supramolecular chirality transformation driven by monodentate ligand binding to a coordinatively unsaturated self-assembly based on C_3-symmetric ligands, *Chem. Sci.*, 2019, **10**, 4236–4245.
24 C. M. Leenders, L. Albertazzi, T. Mes, M. M. Koenigs, A. R. Palmans and E. W. Meijer, Supramolecular polymerization in water harnessing both hydrophobic effects and hydrogen bond formation, *Chem. Commun.*, 2013, **49**, 1963–1965.
25 G. Ghosh, P. Dey and S. Ghosh, Controlled supramolecular polymerization of pi-systems, *Chem. Commun.*, 2020, **56**, 6757–6769.
26 T. F. A. De Greef, M. M. J. Smulders, M. Wolffs, A. P. H. J. Schenning, R. P. Sijbesma and E. W. Meijer, Supramolecular polymerization, *Chem. Rev.*, 2009, **109**, 5687–5754.
27 T. Haino and T. Hirao, Supramolecular polymerization and functions of isoxazolering monomers, *Chem. Lett.*, 2020, **49**, 574–584.
28 N. M. Casellas, S. Pujals, D. Bochicchio, G. M. Pavan, T. Torres, L. Albertazzi and M. Garcia-Iglesias, From isodesmic to highly cooperative: reverting the supramolecular polymerization mechanism in water by fine monomer design, *Chem. Commun.*, 2018, **54**, 4112–4115.
29 J. Kang, D. Miyajima, T. Mori, Y. Inoue, Y. Itoh and T. Aida, A rational strategy for the realization of chain-growth supramolecular polymerization, *Science*, 2015, **347**, 646–651.
30 P. Besenius, G. Portale, P. H. Bomans, H. M. Janssen, A. R. Palmans and E. W. Meijer, Controlling the growth and shape of chiral supramolecular polymers in water, *Proc. Natl. Acad. Sci. U.S.A.*, 2010, **107**, 17888–17893.
31 D. Zhao and J. S. Moore, Nucleation-elongation: a mechanism for cooperative supramolecular polymerization, *Org. Biomol. Chem.*, 2003, **1**, 3471–3491.
32 H. M. M. ten Eikelder, A. J. Markvoort, T. F. A. de Greef and P. A. J. Hilbers, An equilibrium model for chiral amplification in supramolecular polymers, *J. Phys. Chem. B*, 2012, **116**, 5291–5301.
33 G. Vantomme, G. M. Ter Huurne, C. Kulkarni, H. M. M. Ten Eikelder, A. J. Markvoort, A. R. A. Palmans and E. W. Meijer, Tuning the length of cooperative supramolecular polymers under thermodynamic control, *J. Am. Chem. Soc.*, 2019, **141**, 18278–18285.
34 S. Takahashi and S. Yagai, Harmonizing topological features of self-assembled fibers by rosette-mediated random supramolecular copolymerization and self-sorting of monomers by photo-cross-linking, *J. Am. Chem. Soc.*, 2022, **144**, 13374–13383.
35 H. Su, S. A. H. Jansen, T. Schnitzer, E. Weyandt, A. T. Rosch, J. Liu, G. Vantomme and E. W. Meijer, Unraveling the complexity of supramolecular copolymerization dictated by triazine-benzene interactions, *J. Am. Chem. Soc.*, 2021, **143**, 17128–17135.
36 M. J. Mayoral, C. Rest, V. Stepanenko, J. Schellheimer, R. Q. Albuquerque and G. Fernandez, Cooperative supramolecular polymerization driven by metallophilic Pd···Pd interactions, *J. Am. Chem. Soc.*, 2013, **135**, 2148–2151.
37 E. Krieg, H. Weissman, E. Shimoni, A. Bar On and B. Rybtchinski, Understanding the effect of fluorocarbons in aqueous supramolecular polymerization: ultrastrong noncovalent binding and cooperativity, *J. Am. Chem. Soc.*, 2014, **136**, 9443–9452.
38 M. H. Chan, M. Ng, S. Y. Leung, W. H. Lam and V. W. Yam, Synthesis of luminescent platinum(II) 2,6-bis(N-dodecylbenzimidazol-2'-yl)pyridine foldamers and their supramolecular assembly and metallogel formation, *J. Am. Chem. Soc.*, 2017, **139**, 8639–8645.
39 S. Samanta, P. Raval, G. N. Manjunatha Reddy and D. Chaudhuri, Cooperative self-assembly driven by multiple noncovalent interactions: investigating molecular origin and reassessing characterization, *ACS Cent. Sci.*, 2021, **7**, 1391–1399.
40 R. B. Martin, Comparisons of indefinite self-association models, *Chem. Rev.*, 1996, **96**, 3043–3064.
41 M. M. J. Smulders, M. M. L. Nieuwenhuizen, T. F. A. de Greef, P. van der Schoot, A. P. H. J. Schenning and E. W. Meijer, How to distinguish isodesmic from cooperative supramolecular polymerisation, *Chem.–Eur. J.*, 2010, **16**, 362–367.
42 M. A. Martinez, A. Doncel-Gimenez, J. Cerda, J. Calbo, R. Rodriguez, J. Arago, J. Crassous, E. Orti and L. Sanchez, Distance matters: biasing mechanism, transfer of asymmetry, and stereomutation in N-annulated perylene bisimide supramolecular polymers, *J. Am. Chem. Soc.*, 2021, **143**, 13281–13291.
43 H. Choi, S. Ogi, N. Ando and S. Yamaguchi, Dual trapping of a metastable planarized triarylborane pi-system based on

folding and lewis acid-base complexation for seeded polymerization, *J. Am. Chem. Soc.*, 2021, **143**, 2953–2961.
44 Z. Nie, A. Petukhova and E. Kumacheva, Properties and emerging applications of self-assembled structures made from inorganic nanoparticles, *Nat. Nanotechnol.*, 2010, **5**, 15–25.
45 Y. Mai, Z. An and S. Liu, Self-assembled materials and applications, *Macromol. Rapid Commun.*, 2022, **43**, e2200481.
46 H. M. M. Ten Eikelder, B. Adelizzi, A. R. A. Palmans and A. J. Markvoort, Equilibrium model for supramolecular copolymerizations, *J. Phys. Chem. B*, 2019, **123**, 6627–6642.
47 A. Sarkar, R. Sasmal, C. Empereur-Mot, D. Bochicchio, S. V. K. Kompella, K. Sharma, S. Dhiman, B. Sundaram, S. S. Agasti, G. M. Pavan and S. J. George, Self-sorted, random, and block supramolecular copolymers via sequence controlled, multicomponent self-assembly, *J. Am. Chem. Soc.*, 2020, **142**, 7606–7617.
48 R. Katoono, H. Kawai, K. Fujiwara and T. Suzuki, Dynamic molecular propeller: supramolecular chirality sensing by enhanced chiroptical response through the transmission of point chirality to mobile helicity, *J. Am. Chem. Soc.*, 2009, **131**, 16896–16904.
49 M. Karayianni and S. Pispas, Block copolymer solution self-assembly: Recent advances, emerging trends, and applications, *J. Polym. Sci.*, 2021, **59**, 1874–1898.
50 S. Kim, K. Y. Kim, J. H. Jung and S. H. Jung, Supramolecular polymerization based on the metalation of porphyrin nanosheets in aqueous media, *Inorg. Chem. Front.*, 2022, **9**, 1630–1635.
51 X. Li, X. Liu and X. Liu, Self-assembly of colloidal inorganic nanocrystals: nanoscale forces, emergent properties and applications, *Chem. Soc. Rev.*, 2021, **50**, 2074–2101.
52 J. Yeom, P. P. G. Guimaraes, H. M. Ahn, B. K. Jung, Q. Hu, K. McHugh, M. J. Mitchell, C. O. Yun, R. Langer and A. Jaklenec, Chiral supraparticles for controllable nanomedicine, *Adv. Mater.*, 2020, **32**, e1903878.
53 R. Pugliese, F. Fontana, A. Marchini and F. Gelain, Branched peptides integrate into self-assembled nanostructures and enhance biomechanics of peptidic hydrogels, *Acta Biomater.*, 2018, **66**, 258–271.
54 F. Zhang, C. Hu, Q. Kong, R. Luo and Y. Wang, Peptide-/drug-directed self-assembly of hybrid polyurethane hydrogels for wound healing, *ACS Appl. Mater. Interfaces*, 2019, **11**, 37147–37155.
55 W. Song, X. Zhang, Y. Song, K. Fan, F. Shao, Y. Long, Y. Gao, W. Cai and X. Lan, Enhancing photothermal therapy efficacy by in situ self-assembly in glioma, *ACS Appl. Mater. Interfaces*, 2023, **15**, 57–66.
56 J. K. Poon, Z. Chen, S. Y. Leung, M. Y. Leung and V. W. Yam, Geometrical manipulation of complex supramolecular tessellations by hierarchical assembly of amphiphilic platinum(II) complexes, *Proc. Natl. Acad. Sci. U. S. A.*, 2021, **118**, e2022829118.
57 Y. J. Cho, S. Y. Kim, H. J. Son, D. W. Cho and S. O. Kang, Steric effect on excimer formation in planar Pt(ii) complexes, *Phys. Chem. Chem. Phys.*, 2017, **19**, 5486–5494.
58 E. K. Wong, M. H. Chan, W. K. Tang, M. Y. Leung and V. W. Yam, Molecular alignment of alkynylplatinum(II) 2,6-bis(benzimidazol-2-yl)pyridine double complex salts and the formation of well-ordered nanostructures directed by Pt···Pt and donor-acceptor interactions, *J. Am. Chem. Soc.*, 2022, **144**, 5424–5434.
59 T. R. Schulte, J. J. Holstein, L. Krause, R. Michel, D. Stalke, E. Sakuda, K. Umakoshi, G. Longhi, S. Abbate and G. H. Clever, Chiral-at-metal phosphorescent square-planar Pt(II)-complexes from an achiral organometallic ligand, *J. Am. Chem. Soc.*, 2017, **139**, 6863–6866.
60 F. C. Leung, S. Y. Leung, C. Y. Chung and V. W. Yam, Metal-metal and pi-pi interactions directed end-to-end assembly of gold nanorods, *J. Am. Chem. Soc.*, 2016, **138**, 2989–2992.
61 S. Poirier, H. Lynn, C. Reber, E. Tailleur, M. Marchivie, P. Guionneau and M. R. Probert, Variation of M···H-C interactions in square-planar complexes of nickel(II), palladium(II), and platinum(II) probed by luminescence spectroscopy and X-ray diffraction at variable pressure, *Inorg. Chem.*, 2018, **57**, 7713–7723.
62 C. Po, Z. Ke, A. Y. Tam, H. F. Chow and V. W. Yam, A platinum(II) terpyridine metallogel with an L-valine-modified alkynyl ligand: interplay of Pt···Pt, pi-pi and hydrogen-bonding interactions, *Chemistry*, 2013, **19**, 15735–15744.
63 A. Haque, L. Xu, R. A. Al-Balushi, M. K. Al-Suti, R. Ilmi, Z. Guo, M. S. Khan, W. Y. Wong and P. R. Raithby, Cyclometallated tridentate platinum(ii) arylacetylide complexes: old wine in new bottles, *Chem. Soc. Rev.*, 2019, **48**, 5547–5563.
64 C. Y. Sun, W. P. To, F. F. Hung, X. L. Wang, Z. M. Su and C. M. Che, Metal-organic framework composites with luminescent pincer platinum(ii) complexes: (3)MMLCT emission and photoinduced dehydrogenation catalysis, *Chem. Sci.*, 2018, **9**, 2357–2364.
65 G. Park, H. Kim, H. Yang, K. R. Park, I. Song, J. H. Oh, C. Kim and Y. You, Amplified circularly polarized phosphorescence from co-assemblies of platinum(ii) complexes, *Chem. Sci.*, 2019, **10**, 1294–1301.
66 A. Y. Tam, K. M. Wong, G. Wang and V. W. Yam, Luminescent metallogels of platinum(II) terpyridyl complexes: interplay of metal···metal, pi-pi and hydrophobic-hydrophobic interactions on gel formation, *Chem. Commun.*, 2007, **20**, 2028–2030.
67 Q. Wan, X. S. Xiao, W. P. To, W. Lu, Y. Chen, K. H. Low and C. M. Che, Counteranion- and solvent-mediated chirality transfer in the supramolecular polymerization of luminescent platinum(II) complexes, *Angew. Chem., Int. Ed.*, 2018, **57**, 17189–17193.
68 K. Y. Kim, J. Kim, C. J. Moon, J. Liu, S. S. Lee, M. Y. Choi, C. Feng and J. H. Jung, Co-assembled supramolecular nanostructure of platinum(II) complex through helical ribbon to helical tubes with helical inversion, *Angew. Chem., Int. Ed.*, 2019, **58**, 11709–11714.
69 S. G. Kang, K. Y. Kim, Y. Cho, D. Y. Jeong, J. H. Lee, T. Nishimura, S. S. Lee, S. K. Kwak, Y. You and J. H. Jung, Circularly polarized luminescence active supramolecular

nanotubes based on Pt(II) complexes that undergo dynamic morphological transformation and helicity inversion, *Angew. Chem., Int. Ed.*, 2022, **61**, e202207310.

70 M. Kim, M. Ok, C. Li, K. Go, S. Kim, J. Kim, J. H. Jung and S. H. Jung, Supramolecular architectures based on binuclear Pt(ii) complexes consisting of different ligands and circular and helical fiber structures, *Inorg. Chem. Front.*, 2023, **10**, 768–775.

71 J. A. Bailey, M. G. Hill, R. E. Marsh, V. M. Miskowski, W. P. Schaefer and H. B. Gray, Electronic spectroscopy of chloro(terpyridine)platinum(II), *Inorg. Chem.*, 1995, **34**, 4591–4599.

72 V. M. Miskowski, V. H. Houlding, C. Che and Y. Wang, Electronic spectra and photophysics of platinum (II) complexes with -diimine ligands. mixed complexes with halide ligands, *Inorg. Chem.*, 1993, **32**, 2518–2524.

73 I. Eryazici, C. N. Moorefield and G. R. Newkome, Square-planar Pd(II), Pt(II), and Au(III) terpyridine complexes: their syntheses, physical properties, supramolecular constructs, and biomedical activities, *Chem. Rev.*, 2008, **108**, 1834–1895.

74 S. Y. Leung, S. Evariste, C. Lescop, M. Hissler and V. W. W. Yam, Supramolecular assembly of a phosphole-based moiety into nanostructures dictated by alkynylplatinum(ii) terpyridine complexes through non-covalent Pt···Pt and pi-pi stacking interactions: synthesis, characterization, photophysics and self-assembly behaviors, *Chem. Sci.*, 2017, **8**, 4264–4273.

75 M. H. Chan, S. Y. Leung and V. W. W. Yam, Controlling self-assembly mechanisms through rational molecular design in oligo(p-phenyleneethynylene)-containing alkynylplatinum(II) 2,6-bis(N-alkylbenzimidazol-2'-yl) pyridine amphiphiles, *J. Am. Chem. Soc.*, 2018, **140**, 7637–7646.

76 X. Zheng, M. H. Chan, A. K. Chan, S. Cao, M. Ng, F. K. Sheong, C. Li, E. C. Goonetilleke, W. W. Y. Lam, T. C. Lau, X. Huang and V. W. Yam, Elucidation of the key role of Pt···Pt interactions in the directional self-assembly of platinum(II) complexes, *Proc. Natl. Acad. Sci. U. S. A.*, 2022, **119**, e2116543119.

77 M. Ok, K. Y. Kim, H. Choi, S. Kim, S. S. Lee, J. Cho, S. H. Jung and J. H. Jung, Helicity-driven chiral self-sorting supramolecular polymerization with Ag(+): right- and left-helical aggregates, *Chem. Sci.*, 2022, **13**, 3109–3117.

78 S. H. Park, S. H. Jung, J. Ahn, J. H. Lee, K. Y. Kwon, J. Jeon, H. Kim, J. Jaworski and J. H. Jung, Reversibly tunable helix inversion in supramolecular gels trigged by Co(2+), *Chem. Commun.*, 2014, **50**, 13495–13498.

79 P. Pander, A. Sil, R. J. Salthouse, C. W. Harris, M. T. Walden, D. S. Yufit, J. A. G. Williams and F. B. Dias, Excimer or aggregate? near infrared electro- and photoluminescence from multimolecular excited states of N^C^N-coordinated platinum(II) complexes, *J. Mater. Chem. C*, 2022, **10**, 15084–15095.

80 J. Huo, Z. Hu, G. He, X. Hong, Z. Yang, S. Luo, X. Ye, Y. Li, Y. Zhang, M. Zhang, H. Chen, T. Fan, Y. Zhang, B. Xiong, Z. Wang, Z. Zhu and D. Chen, High temperature thermochromic polydiacetylenes: Design and colorimetric properties, *Appl. Surf. Sci.*, 2017, **423**, 951–956.

81 N. Nakashima, S. Asakuma and T. Kunitake, Optical microscopic study of helical superstructures of chiral bilayer membranes, *J. Am. Chem. Soc.*, 1985, **107**, 509–510.